

East Tennessee State University Digital Commons @ East Tennessee State University

Undergraduate Honors Theses

Student Works

5-2013

Numerical study of the effect of blood vessel geometry on plaque formation.

Lindsey Fox

East Tennessee State University

Follow this and additional works at: <https://dc.etsu.edu/honors>



Part of the [Medicine and Health Sciences Commons](#)

Recommended Citation

Fox, Lindsey, "Numerical study of the effect of blood vessel geometry on plaque formation." (2013). *Undergraduate Honors Theses*. Paper 105. <https://dc.etsu.edu/honors/105>

This Honors Thesis - Withheld is brought to you for free and open access by the Student Works at Digital Commons @ East Tennessee State University. It has been accepted for inclusion in Undergraduate Honors Theses by an authorized administrator of Digital Commons @ East Tennessee State University. For more information, please contact digilib@etsu.edu.

*Numerical study of the effect of blood vessel geometry on
plaque formation*

Thesis submitted in partial fulfillment of Honors

By

Lindsey Fox
The Honors College
University Honors, Honors-in-Discipline Mathematics
East Tennessee State University

April 9, 2013

Dr. Anahita Ayasoufi, Mentor

Dr. Michele Joyner, Faculty Reader

Dr. Mallika Dhar, Faculty Reader

ABSTRACT

In the United States, cardiovascular disease is the number one cause of death for both men and women. Heart attacks and strokes can happen because of atherosclerosis, or plaque build-up inside arteries, which obstruct blood flow to the heart and brain. One common site of atherosclerosis is the carotid artery bifurcation. This study looks at how the angle between the branching arteries of the bifurcation affects the potential for atherosclerosis by running flow simulations through virtual models of the bifurcation. The higher the wall shear stress, turbulence intensity, and turbulence kinetic energy at the bifurcation, the lower the chance of atherosclerosis. There is an optimal angle at which this occurs.

TABLE OF CONTENTS

I. Acknowledgements	4
II. Introduction	5
III. Literature Review	6
IV. Method	9
A) Shear Stress	9
i) Shear Stress in Fluids	10
ii) Wall Shear Stress	10
B) Turbulence Intensity and Turbulence Kinetic Energy	11
C) Blood Properties and the Simulation Material	12
D) Governing Equations	13
E) Models	14
F) Pulsatile Flow	15
G) Boundary Conditions	16
H) Flow Simulation	17
V. Data	18
VI. Conclusions	21
VII. Discussion	22
VIII. References	24
IX. Figures	26

I. ACKNOWLEDGEMENTS

I would like to thank the ETSU Honors College for the opportunity to participate in undergraduate research, my faculty readers Dr. Michele Joyner of the Mathematics and Statistics Department and Dr. Mallika Dhar of the Physics and Astronomy Department, Dr. Ramin Rahmani of A.O. Smith Corporation who helped with the simulations, and my faculty thesis advisor Dr. Anahita Ayasoufi of the Mathematics and Statistics Department.

II. INTRODUCTION

In the United States, cardiovascular disease is the number one cause of death for both men and women [6]. It claims approximately one million lives every year [6]. Heart attacks and strokes can happen because of the build-up of fatty materials inside arteries, such as cholesterol, which obstructs blood flow to the heart and brain [14]. This condition is called atherosclerosis [14]. There are numerous causes of atherosclerosis, including an unhealthy diet, smoking, and lack of regular exercise [14]. There are also causes outside of one's control. This study looks at one such possible cause of plaque build-up: the geometry of blood vessels, in particular the angle between branching arteries. In this study, we used the carotid bifurcation as our model. The two common carotid arteries are the principal arteries to supply the head and neck with blood [1]. They each divide into two main branches, the external carotid, which supplies the face and neck, and the internal carotid, which supplies the cranial and orbital cavities in the head [1]. Our study concentrates on the point where the artery divides, i.e., the bifurcation. At this point, an area of low shear stress and low blood flow velocity develops in the artery. These two conditions greatly contribute to atherosclerosis. We built three models of this artery, one at an average angle, one at a wider angle, and one at a narrower angle. Then we ran flow simulations on the models, and analyzed how the angle between the branching arteries affects the shear stress and two other related measures, and thus the potential for atherosclerosis.

III. LITERATURE REVIEW

Many studies have been performed on the carotid arteries, looking at shear stress and flow velocity, but no study has analyzed how the angle between the branching arteries affects shear stress and flow velocity. One such study is in reference [2]. This study investigated the potential role of factors of fluid mechanics in the localized genesis and development of atherosclerotic lesions in humans. They used five isolated human coronary arterial trees to study the exact anatomic locations of atherosclerotic lesions and the flow patterns at the sites of the lesions. Lesions on human vessel walls do not develop randomly and do not occur throughout the entire circulatory system. They localize at certain sites. This study found that atherosclerotic plaques and wall thickenings almost exclusively localize at major bifurcations and T-junctions, especially on the outer walls of the daughter vessels. It was found that in these areas flow was either slow or disturbed, with a separation of streamlines from the vessel wall and formation of eddies, and that the wall shear stress was low. From this study, we decided to measure the wall shear stress, as well as the turbulence intensity and turbulence kinetic energy because of the disturbed flow patterns mentioned. We also took from this study the area where we wanted to take the cross sections of the models. They came from the daughter vessel, just past the bifurcation.

Another study, in reference [9], looked at fluid velocities in a scale model of the human carotid artery, under conditions of pulsatile flow. The flow velocity and wall shear stress were measured and compared with plaque thickness. The study found that wall shear stress was highest in areas where thickness was lowest, which occurred on the inner wall of the daughter vessel. It also found that wall shear stress was lowest in areas where thickness was highest,

which occurred on the outer wall of the daughter vessel. This study confirmed the area from where we wanted to take the cross sections.

The study in reference [10] created a model for intimal thickening to simulate the growth of intima in a carotid bifurcation with a steady flow. They found similar results as references [3] and [9], that thicker intima is formed in regions near the junction and carotid bulb, where flow is more complex, due to low wall shear stress. This result once again confirmed our choice of cross sections. Reference [13] also built a model of blood flow through the carotid artery, but this study considered the fluid-wall interactions. In this study, they make the point that local hemodynamic structure is intimately related to atherogenesis onset and progress. The bifurcation of the carotid artery has the propensity to develop atherosclerotic plaques. In addition, low shear stress regions are associated with the development of plaques. The study found that a region of low flow velocity and low shear stress on the outer wall of the daughter vessel.

One last study, in reference [16], looked at the distribution of intimal plaques in twelve adult human carotid bifurcations. The distribution of the plaques was compared to the distribution of flow streamline patterns, flow velocity profiles, and shear stresses. They found, like the other studies above, that intimal thickening was greatest at the bifurcation, with minimum thickness on the inner wall, and maximum thickness on the outer wall of the daughter vessel. They also found that where the intima was thinnest, flow streamlines were axially aligned and unidirectional, and that where intima was thickest, the pattern of flow was complex and included a region of separation and reversal of axial flow. Wall shear stress was lowest in the regions where the intima was thickest.

Overall, from the studies we know that plaque build-up occurs on the outer wall of the daughter vessel of the bifurcation at the bulb (Figure 7). This is a region of low wall shear stress and slowed, complex flow.

In order to build the models, we needed information on realistic angles between the branching arteries. In reference [9], we found that the average angle is about 50° . In reference [4], we found that the range of angles was very large, and could vary from almost 0° to 100° . From this, we were able to decide on the angles we used for the three models.

IV. METHOD

In this section, I will first discuss the main components involved in our study. This includes shear stress, turbulence intensity, and turbulence kinetic energy, which were the three measures we got data about in the simulations, as well as the properties of blood, which were used to establish a simulation material. Then I will explain the process of the models and simulations. For this, we had to figure out what governing equations would be appropriate, build the bifurcation models, use what we learned from the properties of blood, including the characteristic of pulsatile flow, to determine boundary conditions for the simulations, and determine an appropriate simulation program.

A) Shear Stress

Stress measures the strength of a material when a force is applied to it. It is the force per unit area within materials that arises from externally applied forces. Shear stress, denoted by τ , is the component of stress that is coplanar with a material cross section; the force vector is parallel to the cross section. Shear stress is the opposite of normal stress, where the force vector is perpendicular to the material cross section. The general formula for shear stress is

$$\tau = \frac{F}{A} \quad [1]$$

where F is the force applied and A is the cross-sectional area. Shear stress is measured in Newtons per meter squared (N/m^2), or Pascals.

i) Shear Stress in Fluids

A fluid is a material that changes shape when a force is applied to it. It does not support shear stress, so a fluid at rest has zero shear stress and takes the shape of its container. Any fluid that has a velocity and is moving along a boundary will impress a shear stress on the boundary. For Newtonian fluids in laminar (streamline) flow, the shear stress is proportional to the strain rate. Strain is the measure of deformation of a material due to an externally applied force, and the strain rate is the rate of change in the strain. The constant of proportionality in this relation is the viscosity of the fluid. Viscosity is the measure of a fluid's resistance to flow. The equation for shear stress in fluids is

$$\tau(y) = \mu \frac{\partial u}{\partial y} \quad [2]$$

where μ is the viscosity, u is the velocity of the fluid parallel to the boundary, and y is the height above the boundary. So here, shear stress is a function of the height and is proportional to viscosity and the velocity gradient. One fluid dynamics principle, the no-slip condition, is that at the boundary, the speed of the flow will be zero. At some height from the boundary, the flow will equal the velocity of the fluid. The area in between is the boundary layer. The shear stress on the boundary is due to this loss of velocity. For non-Newtonian fluids, the shear stress is not proportional to the strain rate because the fluid viscosity is not constant.

ii) Wall Shear Stress

Wall shear stress is the integral over the wall of shear stress. The equation is

$$\tau_w = \int \tau(y) dy \quad [3]$$

where $\tau(y)$ is given in equation [2]. In this study, we used one material in the simulations, so we have a given viscosity. The higher the wall shear stress is, the less of a chance there is of plaque

build- up, because there will be a higher velocity gradient, which will detach plaque and carry it away.

B) Turbulence Intensity and Turbulence Kinetic Energy

A turbulent flow is a flow that has chaotic and non-deterministic property changes. It is the opposite of laminar flow. Turbulent eddies, or irregular swirls of motions, create fluctuations in velocity. Turbulence kinetic energy is the mean kinetic energy per unit mass associated with eddies in a turbulent flow, or the strength of the turbulence in the flow. Kinetic energy is given by $KE = \frac{1}{2}mv^2$, where m is mass and v is velocity. Turbulence kinetic energy is similar to kinetic energy, but since turbulence kinetic energy is measured per unit mass, it corresponds to $\frac{1}{2}v^2$. The equation for turbulence kinetic energy is

$$TKE/m = \bar{e} = \frac{1}{2}(\overline{u'^2} + \overline{v'^2} + \overline{w'^2}) = \frac{1}{2}\overline{U'^2} \quad [4]$$

or the sum of the average velocity variances divided by two. The total kinetic energy of the flow is the sum of the kinetic energy of the mean flow and the turbulent flow, $U = \bar{U} + U'$. Turbulent motions associated with eddies are approximately random, so they can be characterized using statistical concepts. Turbulence intensity is a scale expressing turbulence as a percent. Flow with no fluctuations would have a turbulence intensity of 0%. Turbulence intensity is defined as

$$I = \frac{u'}{U} \quad [5]$$

where u' is the standard deviation of the turbulent velocity fluctuations and U is the mean velocity of the flow. The higher the turbulence intensity, the higher the level of mixing in the flow, so there is less of a chance of plaque build-up. Shear stress generates turbulence. The

stronger the shear stress, the stronger the turbulence. This is because the no-slip condition applies to turbulent velocities as well as the mean flow velocity.

C) Blood Properties and the Simulation Material

A fluid is Newtonian if the strain rate and shear stress are proportional, with the proportionality constant being the viscosity of the fluid. That is, the viscosity of the fluid does not depend on the stress state and velocity of the flow. No fluid is perfectly Newtonian, but many fluids can be assumed to be Newtonian, such as water. A non-Newtonian fluid is simply a fluid that differs from Newtonian properties, but mainly it is a fluid that has viscosity that is dependent on the stress state and velocity of the flow. Blood is a non-Newtonian fluid because of the mixture of cells, proteins, lipoproteins, and ions in the fluid. Some of these substances are semisolid particles and thereby increase the viscosity of blood. The material we used for this study is a fluid that has properties between water and blood. It is a Newtonian fluid, like water, since Newtonian fluids are much easier to simulate. But it has the viscosity and density of blood, which gives more accurate and realistic results than water. Blood has a viscosity that is about four times the viscosity of water, but the viscosity is not constant at all flow rates. The Reynolds number (Re) is the ratio of inertial forces to viscous forces in fluids. For blood flow, Re ranges from 1 in small arterioles to 4000 in the largest arteries. This range represents flow where viscous forces are dominant to flow where inertial forces are dominant. In normal pipe flow, turbulence starts around $Re = 2300$. Usually, blood flow is around 1000. But the geometry of blood vessels, among other factors, makes flow turbulent.

D) Governing Equations

Navier-Stokes equations, derived from Newton's second law of momentum conservation applied to fluid motion, describe the motion of fluids. The equations are nonlinear partial differential equations. The general form of the equations of fluid motion is

$$\rho \left(\frac{\partial \mathbf{v}}{\partial t} + \mathbf{v} \cdot \nabla \mathbf{v} \right) = -\nabla p + \nabla \cdot \mathbf{T} + \mathbf{f} \quad [6]$$

where \mathbf{v} is the flow velocity, ρ is the fluid density, p is the pressure, \mathbf{T} is the deviatoric component of the total stress tensor, and \mathbf{f} is the body forces per unit volume acting on the fluid.

The left side of equation [6] describes inertia ($\frac{\partial \mathbf{v}}{\partial t}$ is the unsteady acceleration and $\mathbf{v} \cdot \nabla \mathbf{v}$ is the convective acceleration) and the right side is a summation of body forces and divergence of pressure and stress. The del operator, ∇ , denotes the gradient of a vector field. The del operator is defined as

$$\nabla = \hat{\mathbf{x}} \frac{\partial}{\partial x} + \hat{\mathbf{y}} \frac{\partial}{\partial y} + \hat{\mathbf{z}} \frac{\partial}{\partial z} \quad [7]$$

where $\hat{\mathbf{x}}$, $\hat{\mathbf{y}}$, and $\hat{\mathbf{z}}$ are the unit vectors in their respective directions. The equations dictate velocity rather than position, so a solution is called a velocity field. It describes the velocity of the fluid at a given point in space and time. The total stress tensor is a tensor, or linear map, that describes the state of stress at a point inside a material. So the stress tensor \mathbf{T} takes a direction vector as the input and produces the stress on the surface normal to the vector as the output.

Compressibility is a measure of the relative volume change as a response to pressure; density depends on pressure. Incompressible flow is a flow in which the material density is constant within an infinitesimal volume that moves with the velocity of the fluid. When considering an incompressible flow of a Newtonian fluid, the general Navier-Stokes equations can be simplified since density cancels out. The Navier-Stokes equations for incompressible flow is

$$\rho \left(\frac{\partial \mathbf{v}}{\partial t} + \mathbf{v} \cdot \nabla \mathbf{v} \right) = -\nabla p + \mu \nabla^2 \mathbf{v} + \mathbf{f} \quad [8]$$

where \mathbf{f} still represents the body forces (this includes gravity, which has an effect on blood flow), and μ is viscosity. In the simulations of this study, the Navier-Stokes equations for incompressible flow were used because blood is liquid and will not compress much.

E) Models

Recall from Section III that the average angle of the carotid bifurcation is around 50° and has a broad range. Therefore, we chose 50° as the average angle model, 70° as the wide angle model, and 30° as the narrow angle model. The actual values of the models were 50.61°, 70.13°, and 31.44°, respectively (Figures 1-3). Due to the way the models were built and the angles adjusted, it was nearly impossible to get the angle to be an exact number. To change the angle, we had to move points in the plane with the mouse. A seemingly slight move could result in a drastic change. These values were as close as we could get to the values we wanted.

We built the models using the software SolidWorks. We first built the wide angle model, then adjusted the angle of it to get the other two models. The first step in constructing the model was to create the path of the artery. Since the path is not flat, we had to conduct the construction in a three-dimensional sketch. The path is not straight, so we used a spline tool. To aid the spline function, we built a box to give references for the spline points. After the spline was placed, the spline handles were used to define the right curvature of the artery. The same technique was used to create the branching artery, except the existing spline was also used as a reference point. Next, points were placed along the splines for future placement of the cross sections. Planes were constructed at each of these points that were perpendicular to the spline. Then circular cross sections were created in each plane. The diameter of each cross section was adjusted because the

artery does not have a uniform diameter throughout. The cross sections were then connected using surface lofts. Because this step was done separately for the main artery and the branched artery, the section where the surfaces met needed to be trimmed. Then a fillet was added at the junction to give a smooth transition between the branched artery and the main artery. The last step was to thicken the walls of the artery so it would be a solid body.

Because geometry-based analysis techniques require that the geometry be broken up into a discrete representation, we had to produce meshes for the models before we could run the models through the flow simulation (Figures 4-6). For the simulations, we took a cross section of each model at the daughter vessel, close to the bifurcation (Figures 8-9). We measured the wall shear stress, turbulence intensity, and turbulence kinetic energy of the flow through the cross sections.

F) Pulsatile Flow

The heart pumps blood through the cardiovascular network in a cyclic nature, creating a pulsatile flow, where flow velocity and pressure are unsteady. Blood is pumped out of the heart during systole and rests during diastole. In some arteries, such as the carotid bifurcation, blood flow can be reversed during diastole, when the pressure is zero or close to zero. In the flow simulations, we ran the simulations twice for each model and measure, one with up flow and one with down flow to account for this reversal of flow. Figure 28 shows modeled blood flow through the carotid bifurcation. A unique feature of the carotid bifurcation is the bulb at the beginning of the internal carotid artery. "The main stream moves upward along the centerline and flow divider along the posterior wall... counter-rotating secondary vortices move upstream toward the common carotid in a separation region," [8]. This upstream movement toward the

common carotid is the reversal of flow during diastole. It is on the outer wall of the bulb where the reversal occurs, contributing to the flow velocity fluctuations and low shear stress in this area.

G) Boundary Conditions

For the simulation, we needed boundary conditions to solve the Navier-Stokes equations. These boundaries help direct the motion of flow, and describe the entrance and exit of the flow. One boundary condition we used was the no-slip condition, where the velocity of the flow is zero at the wall of the blood vessel. For the inlet conditions, we had a constant mass flow rate based on the peaks of the pulsatile flow data from reference [9], we set the turbulence intensity, pressure was calculated, and we had a fully developed velocity profile. For the outlet conditions, the pressure was calculated, and we had zero diffusion flux and overall mass balance. The last two outlet conditions are set to make sure that the amount of fluid going through the simulation is the same going in the vessel and coming out of the vessel. Since the flow is pulsatile, we extracted input flow rate points from a table in [9], and fitted a formula to them using Matlab. For the curve fit, a 4-term Fourier fit was used. Figure 29 is an image of the fitted curve. On the curve, there is a main maximum and a main minimum. These correspond to the up flow and down flow, respectively, discussed in Section H.

H) Flow Simulation

Once the models were built and the boundary conditions were set, the flow simulations could be run. In the simulation, the program used was a Navier-Stokes solver with K-Omega turbulence modeling. The K-Omega model is a two-equation model that represents the turbulent

properties of flow. It determines the scale and energy of the turbulence. The simulation used the SIMPLE algorithm as the Navier-Stokes solver, and coupled pressure and velocity. SIMPLE stands for Semi-Implicit Method for Pressure Linked Equations. According to [12], the basic steps of the algorithm are:

- "1. Set the boundary conditions.
2. Compute the gradients of velocity and pressure.
3. Solve the discretized momentum equation to compute the intermediate velocity field.
4. Compute the uncorrected mass fluxes at faces.
5. Solve the pressure correction equation to produce cell values of the pressure correction.
6. Update the pressure field.
7. Update the boundary pressure corrections.
8. Correct the face mass fluxes.
9. Correct the cell velocities.
10. Update density due to pressure changes."

The algorithm is iterative. "An approximation of the velocity field is obtained by solving the momentum equation. The pressure gradient term is calculated using the pressure distribution from the previous iteration or an initial guess. The pressure equation is formulated and solved in order to obtain the new pressure distribution. Velocities are corrected and a new set of conservative fluxes is calculated [12]."

V. DATA

In the simulations, we had three artery models, a narrow angle, an average angle, and a wide angle. We looked at three measures, turbulence intensity, turbulence kinetic energy, and wall shear stress. For each model and measure, we ran two simulations, one with down flow and one with up flow, to account for the reversal of flow discussed in the Section IV, C. The data from simulations are in the Tables 1-3 and images of the results are in Figures 10-27.

Table 1.

TURBULENCE INTENSITY (%)				
	Overall		On the Wall	
Angle	Down Flow	Up Flow	Down Flow	Up Flow
Narrow	0.02286	0.09923	0.0026	0.055
Average	0.05128	0.13128	0.0056	0.096
Wide	0.03458	0.13365	0.0046	0.067

Table 2.

TURBULENCE KINETIC ENERGY (J/kg)				
	Overall		On the Wall	
Angle	Down Flow	Up Flow	Down Flow	Up Flow
Narrow	0.00079	0.01478	0.0000189	0.0055
Average	0.00395	0.02585	0.00000037	0.01495
Wide	0.00179	0.02679	0.000000022	0.0079

Table 3.

WALL SHEAR STRESS (Pa)				
	Overall		On the Wall	
Angle	Down Flow	Up Flow	Down Flow	Up Flow
Narrow	3.31586	14.9007	1.82	13.42
Average	2.56262	15.1834	2.53	14.48
Wide	2.60467	13.2492	2.59	13.09

In our analysis of the data, there were two main considerations. One involved the up flow and down flow simulations. Since up flow is what mostly occurs in the carotid artery (arteries move blood away from the heart, which would be in an up direction, toward the head, in the carotid arteries) and down flow represents the reversal of flow, we considered the up flow simulations as the more important outcomes. The up flow results also showed a more drastic change between the models. The second consideration involved was where in the cross section of the artery the data came from. It was important to this study to not just consider the data from the overall cross section, but the data that came from the wall of the cross section, since this is where plaque build-up occurs.

When the wall and the up flow is taken into consideration, the highest values for all three measures occurs in the average angle model. The lowest values of turbulence intensity and turbulence kinetic energy occurs in the narrow angle model, and the lowest value of the wall shear stress occurs in the wide angle model. Figures 30-38 are images of the wall of the cross sections for each of the measures in the up flow simulations. Tables 4-9 show the percent difference between each model for each measure.

Table 4.

Percent Difference, Turbulence Intensity, Up Flow, Overall		
	Narrow Angle	Average Angle
Narrow Angle	---	---
Average Angle	27.81%	---
Wide Angle	29.56%	1.79%

Table 5.

Percent Difference, Turbulence Intensity, Up Flow, On the Wall		
	Narrow Angle	Average Angle
Narrow Angle	---	---
Average Angle	54.31%	---
Wide Angle	19.67%	35.58%

Table 6.

Percent Difference, Turbulence Kinetic Energy, Up Flow, Overall		
	Narrow Angle	Average Angle
Narrow Angle	---	---
Average Angle	54.49%	---
Wide Angle	57.78%	3.57%

Table 7.

Percent Difference, Turbulence Kinetic Energy, Up Flow, On the Wall		
	Narrow Angle	Average Angle
Narrow Angle	---	---
Average Angle	92.42%	---
Wide Angle	35.82%	61.71%

Table 8.

Percent Difference, Wall Shear Stress, Up Flow, Overall		
	Narrow Angle	Average Angle
Narrow Angle	---	---
Average Angle	1.88%	---
Wide Angle	11.73%	13.61%

Table 9.

Percent Difference, Wall Shear Stress, Up Flow, On the Wall		
	Narrow Angle	Average Angle
Narrow Angle	---	---
Average Angle	7.59%	---
Wide Angle	2.49%	10.08%

VI. CONCLUSIONS

When we first started this study, we hypothesized that the narrower the angle between the branching arteries, the higher the turbulence intensity, turbulence kinetic energy, and wall shear stress, and thus the lower the chance of atherosclerosis. The first two simulations we ran were on the wide angle and average angle models. The data from these two simulations led us to believe that our hypothesis was correct. However, when the data came back from the simulation on the narrow angle model, it was clear that our hypothesis needed to be revised. The highest values of all three measures occurred in the average angle model, indicating that the least chance of atherosclerosis occurs when the branching arteries are about 50° apart. This means that instead the lowest angle being best, there is an optimal angle at which the three measures are highest.

VII. DISCUSSION

The end goal of our study is to enhance current knowledge of cardiovascular disease. Ultimately, doctors would be able to look at images of the carotid arteries, or other blood vessels, from MRIs and other imaging devices, and determine if a patient is at risk for heart disease. With this knowledge of potential risk, a patient could modify diet and lifestyle to counteract this risk factor. If a doctor had this capability, deaths from cardiovascular disease could be decreased.

The next step in this study would be to find the exact optimal angle. This might require a different construction method for the models so that the exact angle could be entered. We are continuing the study on the theoretical reason behind the existence of an optimal angle, instead of the lowest angle being best. There would have to be something about a narrower angle that slows the flow or obstructs the unidirectional, streamline flow. We are currently working to figure this out. Also, the data from the narrow angle simulation could be misleading. The cross section from the narrow angle model actually extended into the main vessel a bit. (This is the reason why the images of the results of the narrow angle model are not circular.)

Further work that could be done with this project would include using a more accurate and realistic material that has more similar properties to blood. One of these properties to consider would be a material that is non-Newtonian. We chose to use a Newtonian material because it is good for qualitative comparisons, which was the intended outcome of this study, rather than exact quantitative results. Also, if we had used a non-Newtonian material, we would not have been able to use the K-Omega model and the simulations would have taken more computing time. Another property to consider would be the elastic property of vessels. Other aspects of the vessel geometry could be tested as well, such as the cross sectional shape of the

vessel. In our models, the cross sections were circular. Other measures of fluid dynamics besides shear stress, turbulence intensity, and turbulence kinetic energy could be tested in the flow simulations too. Overall, future work on this project would involve making the models and simulation more life-like.

VIII. REFERENCES

- [1] "The Arteries of the Head and Neck: The Common Carotid Artery." *Human Anatomy*. N.p., n.d. Web. 1 Dec. 2012. <http://www.theodora.com/anatomy/the_common_carotid_artery.html>.
- [2] Asakura, T., and T. Karino. "Flow Patterns and Spatial Distribution of Atherosclerotic Lesions in Human Coronary Arteries." *Journal of the American Heart Association* 66 (1990): 1045-066. Web.
- [3] *Biomedical Engineering Branched Vein Tutorial*. SolidWorks, 2012. YouTube.
- [4] Fisher, M., and S. Fieman. "Geometric Factors of the Bifurcation in Carotid Atherogenesis." *Journal of the American Heart Association: Stroke* 21 (1990): 267-71. *American Heart Association*. Web. 15 Mar. 2013. <<http://stroke.ahajournals.org/content/21/2/267.full.pdf>>.
- [5] "Geometry of Blood Vessels May Influence Heart Disease." *ScienceDaily*. N.p., 4 Sept. 1998. Web. <<http://www.sciencedaily.com/releases/1998/09/980904035915.htm>>.
- [6] "Heart Disease: Scope and Impact." *The Heart Foundation*. N.p., 2012. Web. 1 Dec. 2012. <<http://www.theheartfoundation.org/heart-disease-facts/heart-disease-statistics/>>.
- [7] Huo, Yunlong, and Ghassan S. Kassab. "Pulsatile Blood Flow in the Entire Coronary Arterial Tree: Theory and Experiment." *AJP- Heart and Circulatory Physiology* 291 (2006): H1074-1087. Web.
- [8] Ku, David N. "Blood Flow in Arteries." *Annual Reviews, Fluid Mechanics* 29 (1997): 399-434. *Annual Reviews Inc*. Web. 29 Apr. 2013.
- [9] Ku, D. N., D. P. Giddens, C. K. Zarins, and S. Glagov. "Pulsatile Flow and Atherosclerosis in the Human Carotid Bifurcation, Positive Correlation Between Plaque Location and Low Oscillating Shear Stress." *Journal of the American Heart Association* 5 (1985): 293-302. Web.
- [10] Lee, D., and J. J. Chiu. "Intimal Thickening Under Shear in a Carotid Bifurcation- A Numerical Study." *Journal of Biomechanics* 29.1 (1996): 1-11. *Elsevier Science Ltd*. Web.
- [11] Rieutord, Thibault. *Navier-Stokes 1D Model for Blood Flow Simulations in a Vascular Network*. Tech. N.p.: n.p., n.d. Print.
- [12] "SIMPLE [Semi-Implicit Method for Pressure-Linked Equations]." *CFD Online*. N.p., 28 Dec. 2011. Web. 29 Apr. 2013. <http://www.cfd-online.com/Wiki/SIMPLE_algorithm>.
- [13] Urquiza, Santiago, Pablo Blanco, Guillermo Lombera, Marcelo Venere, and Raul Feijoo. "Coupling Multidimensional Compliant Models for Carotid Artery Blood Flow." *Mecanica Computacional XXII* (2003): n. pag. Web.

[14] "What Causes a Heart Attack?" *National Heart Lung and Blood Institute*. National Institutes of Health, 1 Mar. 2011. Web. 1 Dec. 2012. <<http://www.nhlbi.nih.gov/health/health-topics/topics/heartattack/causes.html>>.

[15] "What Is Atherosclerosis?" *WebMD*. WebMD, n.d. Web. 1 Dec. 2012. <<http://www.webmd.com/heart-disease/what-is-atherosclerosis>>.

[16] Zarins, C. K., D. P. Giddens, B. K. Bharadvaj, V. S. Sottiurai, R. F. Mabon, and S. Glagov. "Carotid Bifurcation Atherosclerosis, Quantitative Correlation of Plaque Localization with Flow Velocity Profiles and Wall Shear Stress." *Journal of the American Heart Association* 1983.53 (1983): 502-14. Web.

IX. FIGURES

Figure 1.
Narrow angle model

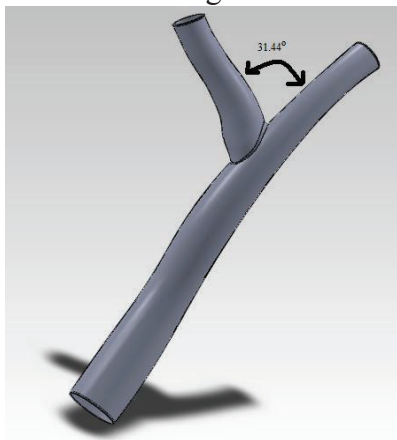


Figure 2.
Average angle model

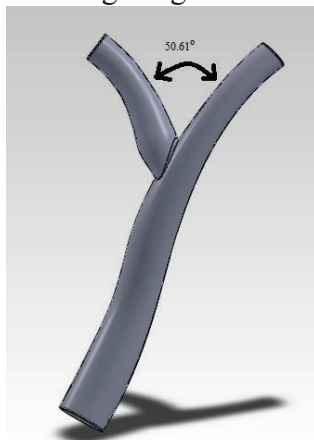


Figure 3.
Wide angle model

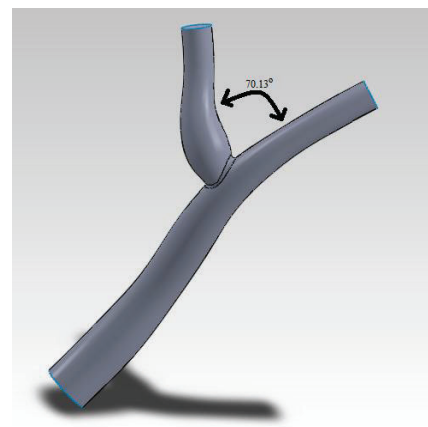


Figure 4.
Example of the mesh

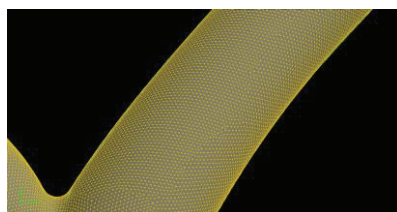


Figure 5.
Example of the mesh

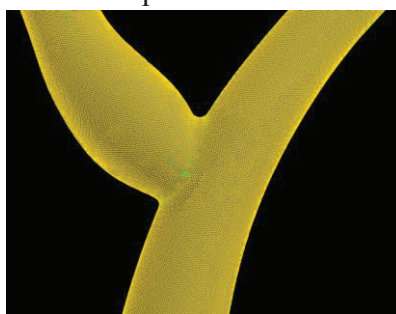


Figure 6.
Example of the mesh

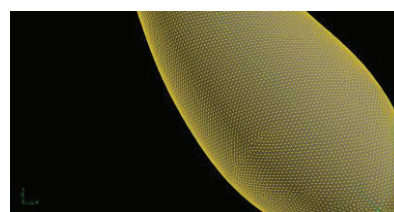


Figure 7. Outer wall of the daughter vessel at the bulb

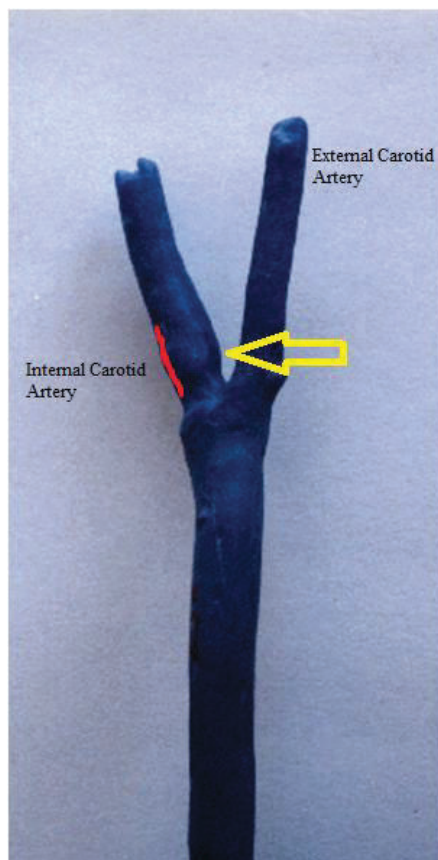


Figure 8.
Cross section

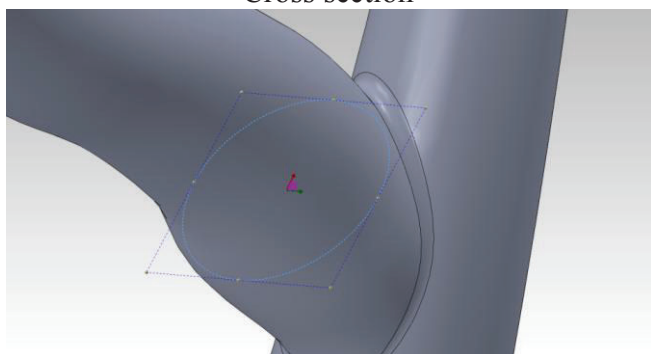


Figure 9.
Cross section

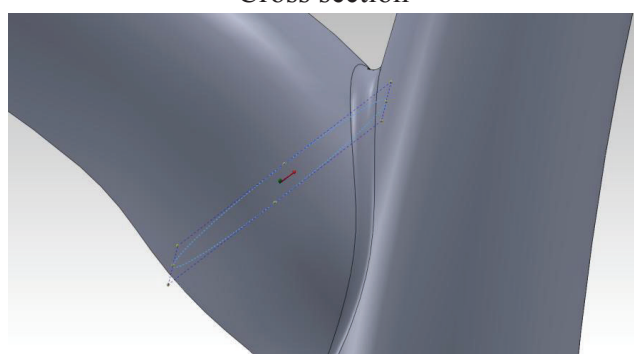
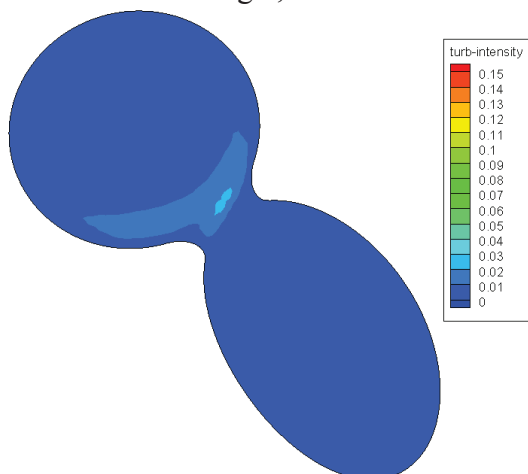
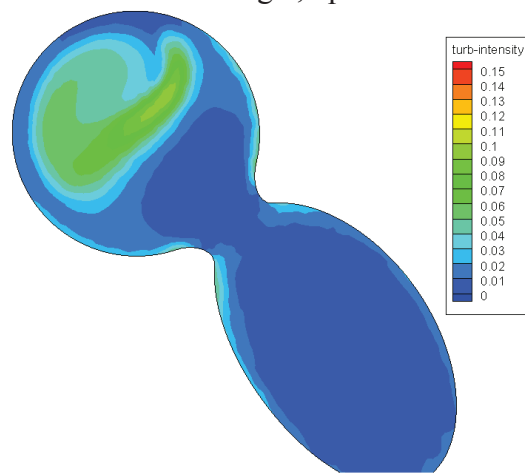


Figure 10.

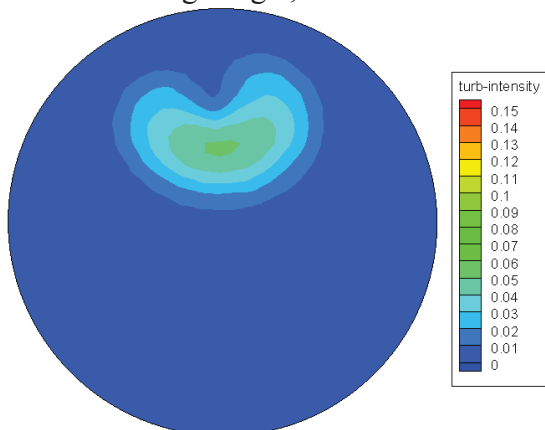
Cross section of results, turbulence intensity,
narrow angle, down flow

**Figure 11.**

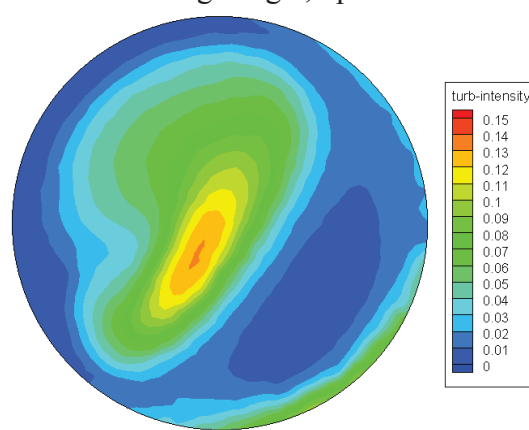
Cross section of results, turbulence intensity,
narrow angle, up flow

**Figure 12.**

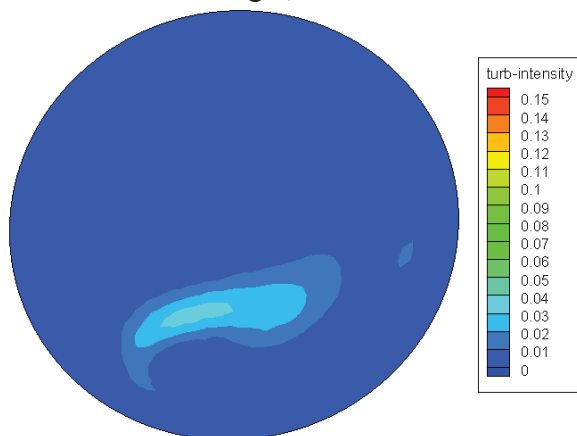
Cross section of results, turbulence intensity,
average angle, down flow

**Figure 13.**

Cross section of results, turbulence intensity,
average angle, up flow

**Figure 14.**

Cross section of results, turbulence intensity,
wide angle, down flow

**Figure 15.**

Cross section of results, turbulence intensity,
wide angle, up flow

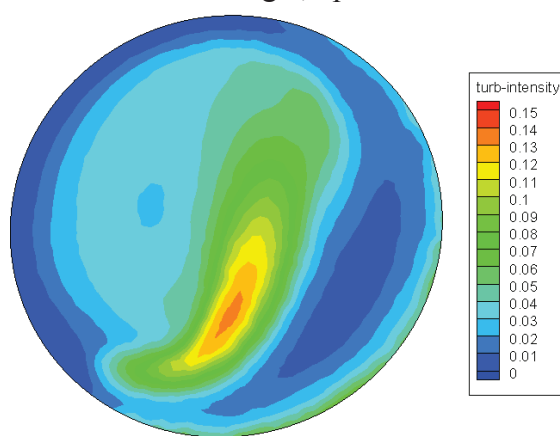
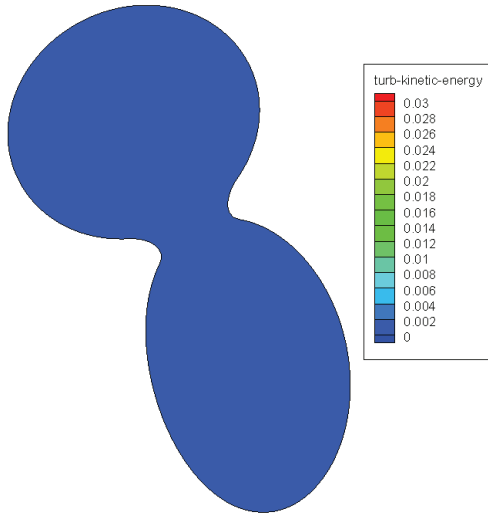
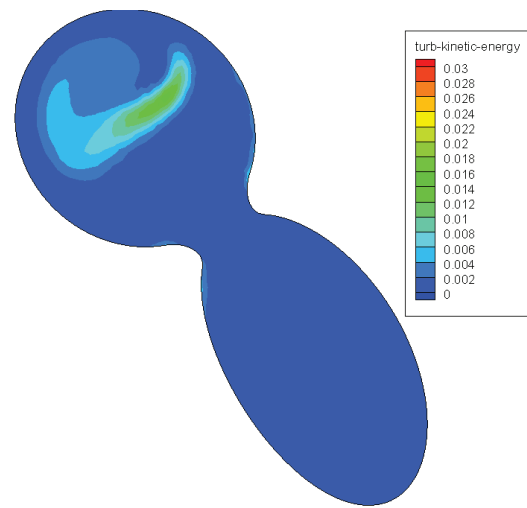


Figure 16.

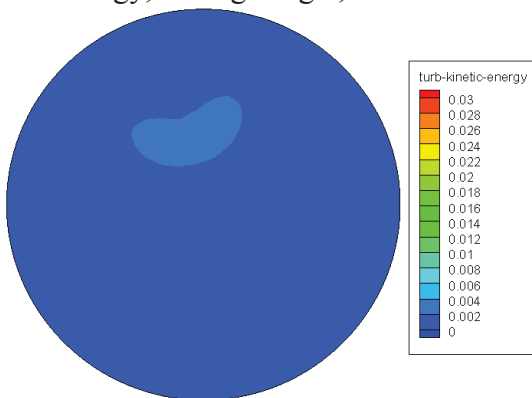
Cross section of results, turbulence kinetic energy, narrow angle, down flow

**Figure 17.**

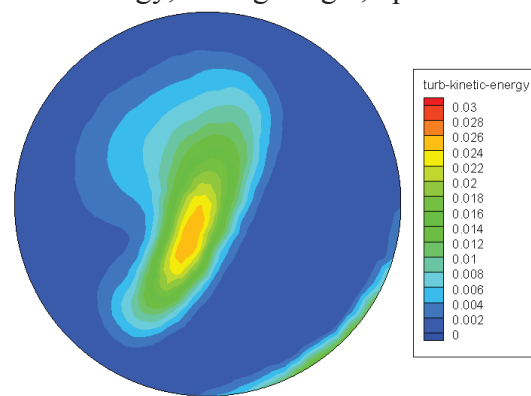
Cross section of results, turbulence kinetic energy, narrow angle, up flow

**Figure 18.**

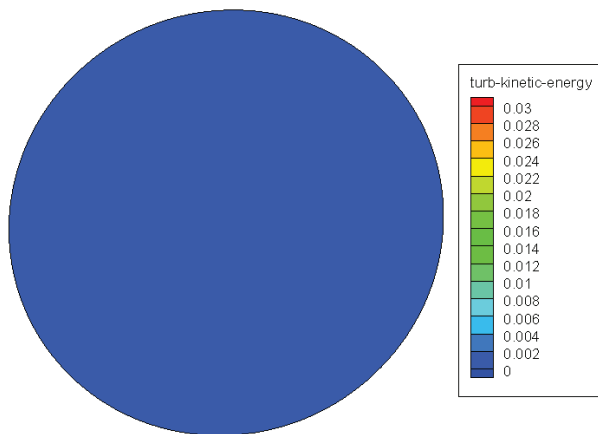
Cross section of results, turbulence kinetic energy, average angle, down flow

**Figure 19.**

Cross section of results, turbulence kinetic energy, average angle, up flow

**Figure 20.**

Cross section of results, turbulence kinetic energy, wide angle, down flow

**Figure 21.**

Cross section of results, turbulence kinetic energy, wide angle, up flow

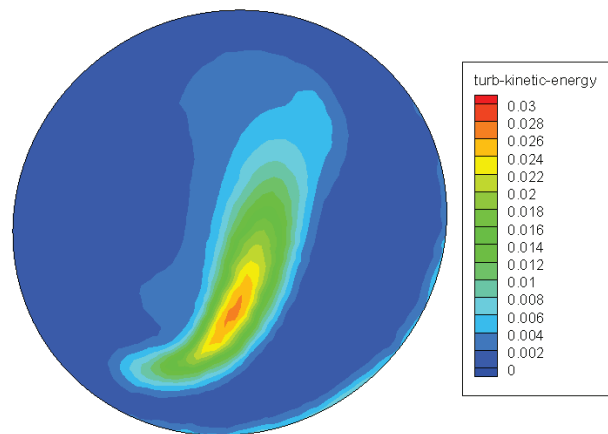
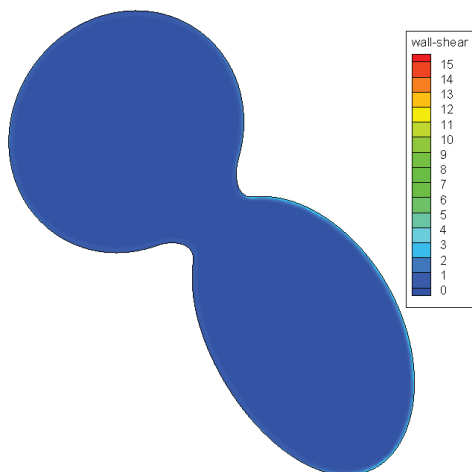
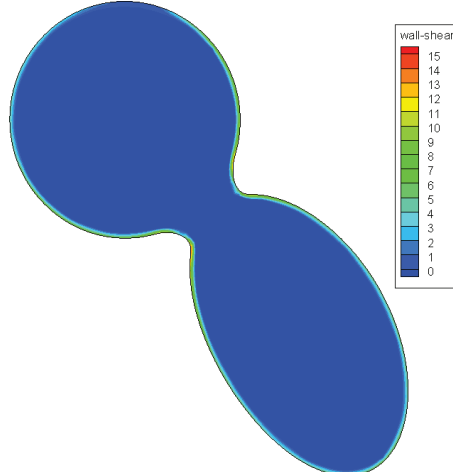


Figure 22.

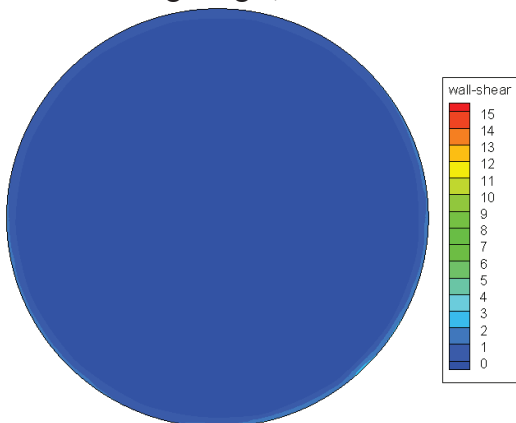
Cross section of results, wall shear stress,
narrow angle, down flow

**Figure 23.**

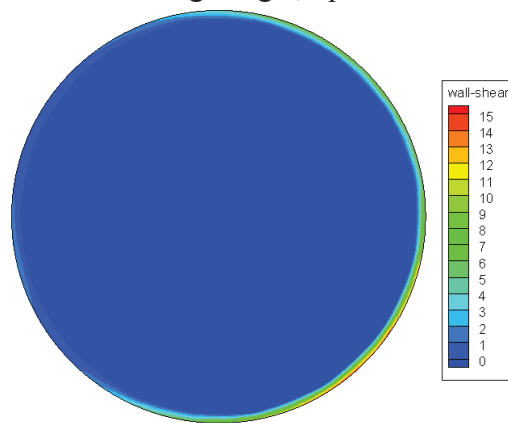
Cross section of results, wall shear stress,
narrow angle, up flow

**Figure 24.**

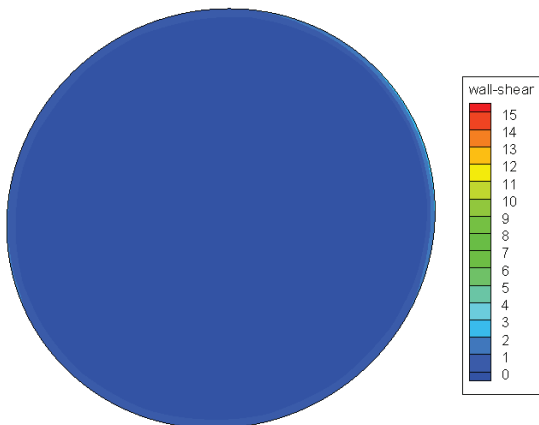
Cross section of results, wall shear stress,
average angle, down flow

**Figure 25.**

Cross section of results, wall shear stress,
average angle, up flow

**Figure 26.**

Cross section of results, wall shear stress, wide
angle, down flow

**Figure 27.**

Cross section of results, wall shear stress, wide
angle, up flow

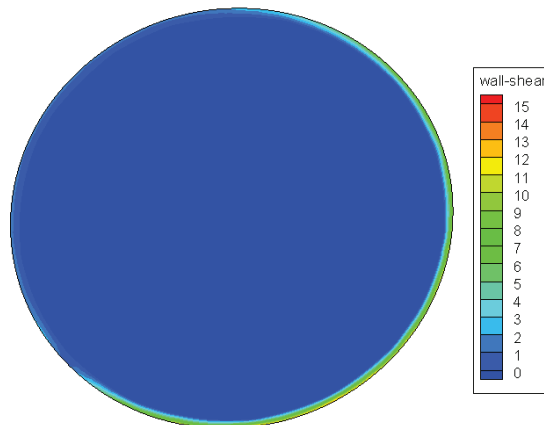


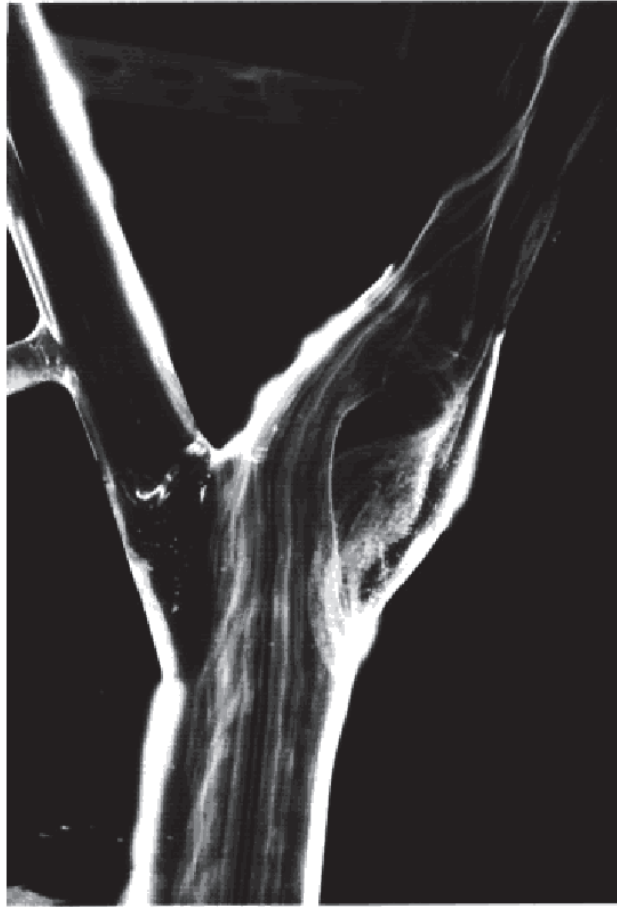
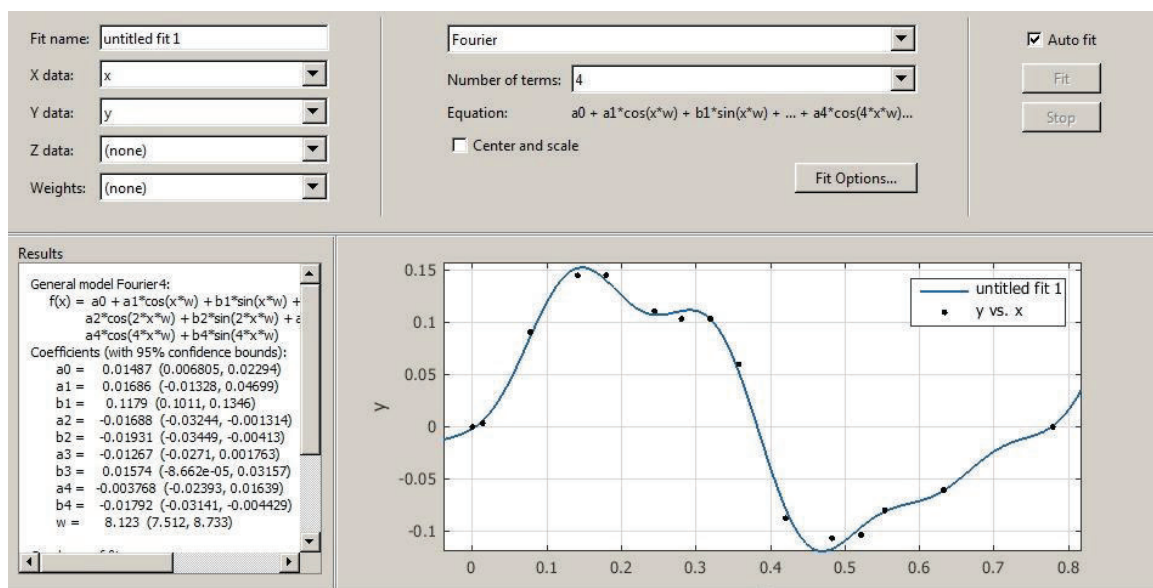
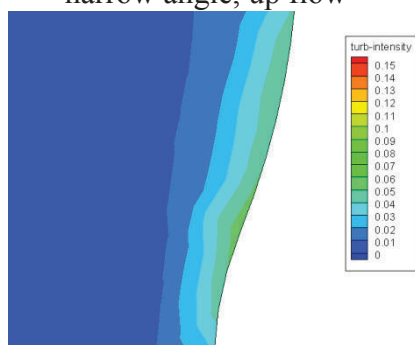
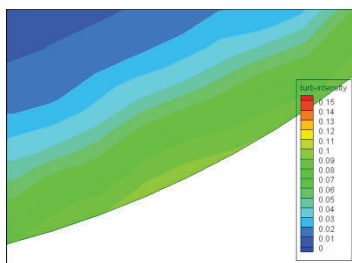
Figure 28. Modeled flow in the carotid artery bifurcation**Figure 29.** Fourier fit curve for input flow rate.

Figure 30.

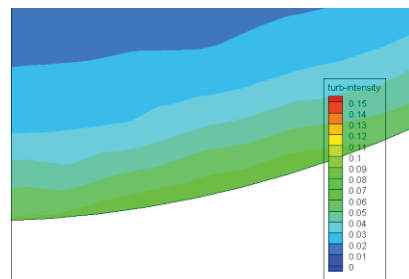
Close up of wall of cross section, turbulence intensity, narrow angle, up flow

**Figure 31.**

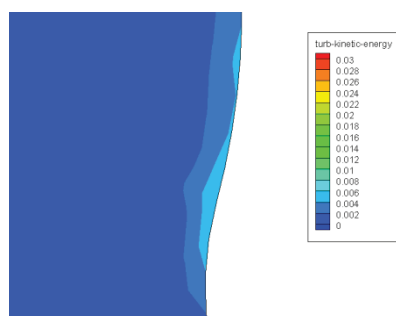
Close up of wall of cross section, turbulence intensity, average angle, up flow

**Figure 32.**

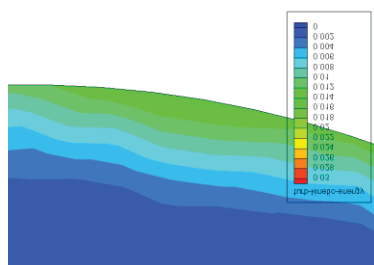
Close up of wall of cross section, turbulence intensity, wide angle, up flow

**Figure 33.**

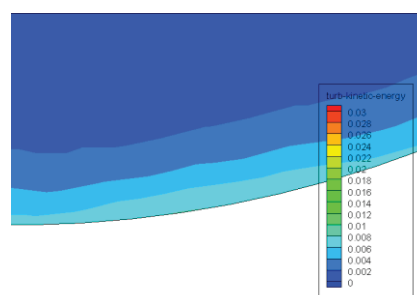
Close up of wall of cross section, turbulence kinetic energy, narrow angle, up flow

**Figure 34.**

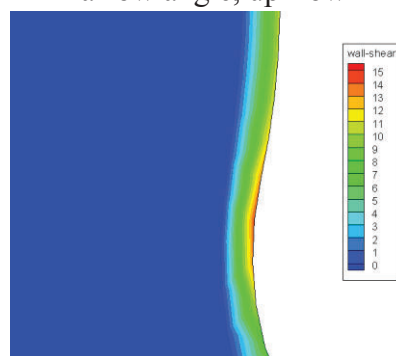
Close up of wall of cross section, turbulence kinetic energy, average angle, up flow

**Figure 35.**

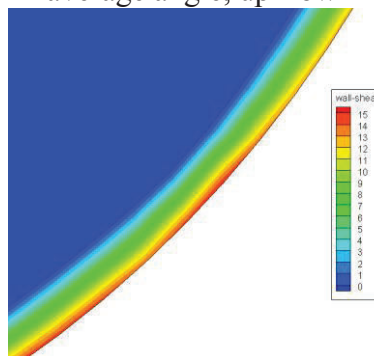
Close up of wall of cross section, turbulence kinetic energy, wide angle, up flow

**Figure 36.**

Close up of wall of cross section, wall shear stress, narrow angle, up flow

**Figure 37.**

Close up of wall of cross section, wall shear stress, average angle, up flow

**Figure 38.**

Close up of wall of cross section, wall shear stress, wide angle, up flow

